Computer Aided Detection/Computer Aided Classification and Data Fusion Algorithms for Automated Detection and Classification of Underwater Mines

Charles M. Ciany
Jim Huang
Raytheon Systems Company
1847 West Main Road
Portsmouth, RI 02871-1087

Abstract- **Raytheon has successfully developed a computer-aided detection/computer aided classification (CAD/CAC) algorithm to process the sidescan sonar outputs of both the AN/AQS-20 helicopter-towed minehunting system and Woods Hole Oceanographic Institute's (WHOI) Remote Environmental Monitoring UnitS (REMUS) unmanned underwater vehicle. These systems employ high frequency acoustic imaging sonars to detect, classify, and localize minelike objects on the ocean bottom. The algorithm was initially demonstrated at the Coastal System Station (CSS) underwater range in Panama City, Florida, and then applied to REMUS sonar imagery taken in the Very Shallow Water (VSW) environment off the coast of San Diego, California. A data fusion technique for combining the outputs of three different CAD/CAC algorithms was subsequently developed and applied to a set of REMUS data. The fusion demonstrated a 4:1 reduction in false alarms relative to any single CAD/CAC algorithm. This paper gives overviews of the AN/AQS-20 and the REMUS systems, describes the Raytheon CAD/CAC and Data Fusion algorithms, and gives sample results from processing of the sea test data.**

I. AN/AQS-20 SYSTEM OVERVIEW

The AN/AQS-20 airborne minehunting sonar system is designed to provide real-time detection and classification of bottom mines, close-tethered mines, near-surface mines, and volume mines at significantly higher search rates than currently deployed systems. To meet these difficult mission requirements, the system integrates five separate sonars in a single towed body cabled to the Navy's MH-53E helicopter. Fig. 1 depicts the system in operation. The five sonars are a Forward-Looking Sonar (FLS), a Volume-Search Sonar (VSS), a Gap-Filler Sonar (GFS) and two (port and starboard) Side-Looking Sonars (SLS). The AN/AQS-20 is capable of performing a search in any of six different modes, each of which uses from one to four of the sonars concurrently. Two of these six modes provide a single-pass search capability. Fig. 2 shows the various sonar operating modes.

Shown in Fig. 3, the AN/AQS-20 must meet a set of demanding space and weight requirements by employing a dense packing design that utilizes both ceramic and polymer transducer technology. Its hydrodynamic design incorporates a closed-loop stabilization technique, which allows it to be towed at the required forward speed while maintaining either a constant depth or constant altitude, depending on the selected operating mode.

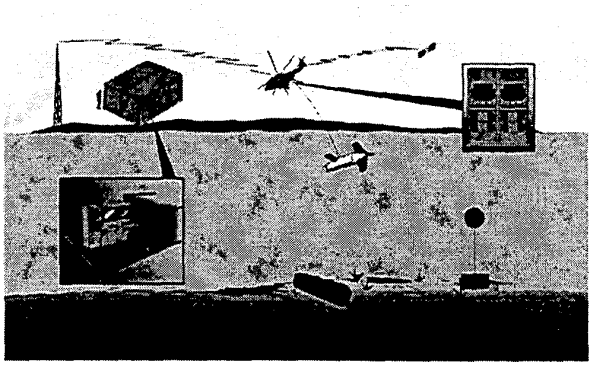

Fig. 1. Raytheon's AN/AQS-20 airborne minehunting sonar

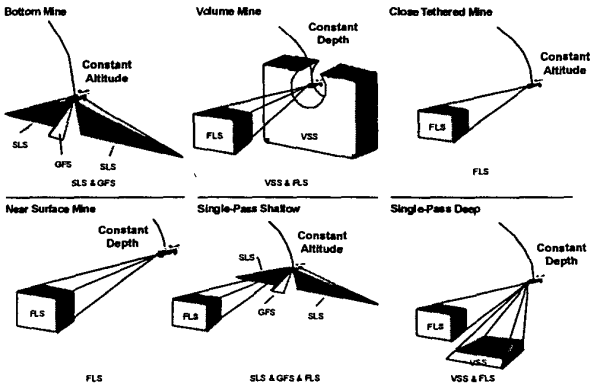

Fig. 2. AN/AQS-20 search modes

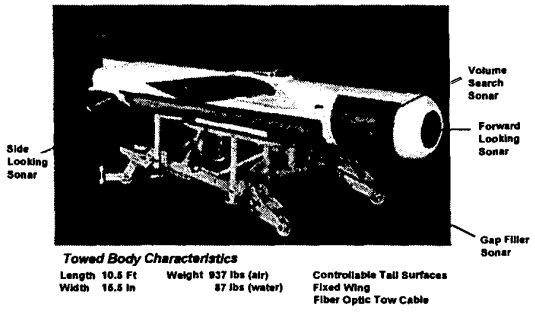

Fig. 3. AN/AQS-20 towed body

II. REMUS SYSTEM OVERVIEW

Shown in Fig. 4, REMUS is a compact, low cost underwater unmanned vehicle (UUV) based on commercial off-the-shelf (COTS) technology and designed by WHOI for coastal monitoring and multiple vehicle survey operations. An unmodified REMUS vehicle is 54 inches long with a body diameter of 7.5 inches. The vehicle's length may be increased to support specific application payloads. The current design weighs 64 pounds in air, and may be trimmed for operations in fresh or salt water. The vehicle can be programmed to run at a specified depth or altitude off of the bottom. The main REMUS subsystems are: *1) Vehicle Power System,* which supplies 44 watt-hours/kilogram of electrical power through sealed, rechargeable lead acid batteries; *2) Compass and Attitude Sensor* that provides 10 Hz rate updates; *3) Pressure Sensor*; *4) Test hardware* to monitor vehicle power and detect leaks before launch; *5) Motors*, each controlled by a dedicated microcontroller that communicates with the main CPU via a shared serial data bus; *6) Acoustic System* to provide both Ultra Short BaseLine (USBL) and Long BaseLine (LBL) acoustic navigation using wideband pulsed waveforms for reliable performance in very shallow water; and *7) Scientific Payload* including an upward and downward looking Acoustic Doppler Current Profiler (ADCP), a Conductivity-Temperature-Depth (CTD) sensor, a Light Scattering Sensor to measure water turbidity and suspended particulate matter, a 600 kHz Side-scan Sonar providing high resolution images of the bottom, and an altimeter to provide the vehicle with a low cost bathymetry capability. The vehicle has been upgraded to support autonomous docking.

III. COMPUTER AUTOMATED DETECTION/COMPUTER AUTOMATED CLASSIFICATION (CAD/CAC) OF MINES

In the early 1990's, Raytheon developed [1] an Image Understanding System for the analysis of the content of high-frequency sonar imagery and later applied it to form the processing for automated detection and classification of mines for the AN/AQS-20 helicopter-towed minehunting system. In this application, the CAD/CAC processing is applied to the SLS and GFS sonar data streams. In early Navy evaluations using data from the earlier AN/AQS-14 system, the minehunting CAD/CAD system demonstrated superior detection and false alarm performance relative to competing automated recognition systems. In more recent system tests, the CAD/CAC processing flow of Fig. 5 has been successfully demonstrated on actual bottom and moored mines at the CSS shallow water range, including the difficult Manta and Rockan mines.

Fig. 4. REMUS vehicle with internal payload

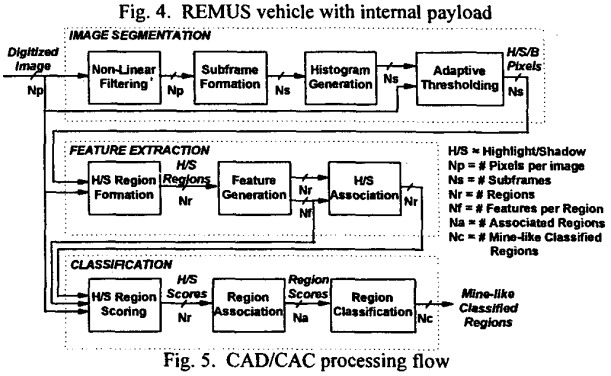

Fig. 5. CAD/CAC processing flow

The CAD/CAC processing consists of three primary functions:

1. ***Image Segmentation***, in which the digitized sidescan sonar image is median filtered to reduce speckle. The image is then split into overlapping range segments ("subframes"), each of which is adaptively thresholded (via pixel histograms) to identify Highlight (high pixel values), Shadow (low pixel values), and Background (remaining pixels) pixel types;

2) ***Feature Extraction***, in which the Highlight/Shadow pixels of each image segment are geometrically associated to form contiguous Highlight/Shadow regions of interest, each of which are processed to extract key Signal, Signal-to-Noise Ratio (SNR), and geometric shape features (e.g. area, perimeter); and

3) ***Classification*** of each region as mine-like or non-mine-like through the association of the individual Highlight/Shadow regions, a weighted scoring of the associated features, and subsequent thresholding of the weighted scores.

IV. AN/AQS-20 SEA TRIAL RESULTS

Initial field testing of the AN/AQS-20 system in July 1997 at the CSS underwater range in Panama City demonstrated an impressive SLS image quality, as illustrated by the examples of Figs. 6 and 7. These examples are extracted from the starboard-looking sonar images, and show the details of a sunken shipwreck. Each of the images shown is presented at a 1:1 aspect ratio.

Fig. 6. AN/AQS-20 SLS image of sunken shipwreck at starboard aspect

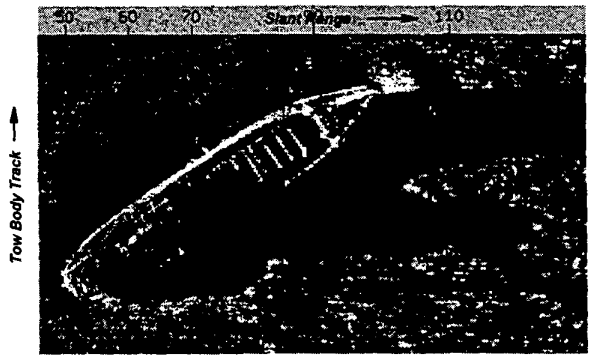

Fig. 7. AN/AQS-20 SLS image of sunken shipwreck at near-stern aspect

Following the initial sea trials, the CAD/CAC parameters and image processing algorithms were adjusted based on findings of sea data analysis performed at Raytheon's AN/AQS-20 laboratory in Portsmouth, Rhode Island. Upon completion of the data analysis, the system was returned to the CSS shallow water minefield in June 1998 for testing with the modified CAD/CAC software.

Fig. 8 shows a detailed layout of the minefield at CSS, indicating the locations of the bottom mines relative to five different helicopter test tracks. A total of 28 targets are in the minefield. The tracks are each oriented along 135 degrees relative to due east, and spaced 50 yards apart.

An analysis of the June 1998 test results shows that the CAD/CAC algorithm successfully detected and classified the bottom mines as mine-like. Five different test runs (designated HS210, HS220, HS230, HS240, and HS250) were executed with the helicopter flying along test tracks 1 and 3. Note that several of the mine targets (Mk 6, Mk 25, Mk 55, Mk 56, and Mk 57) were correctly detected and classified on all test opportunities, while the more challenging Manta and Rockan mines were successfully detected and classified on half of the test opportunities.

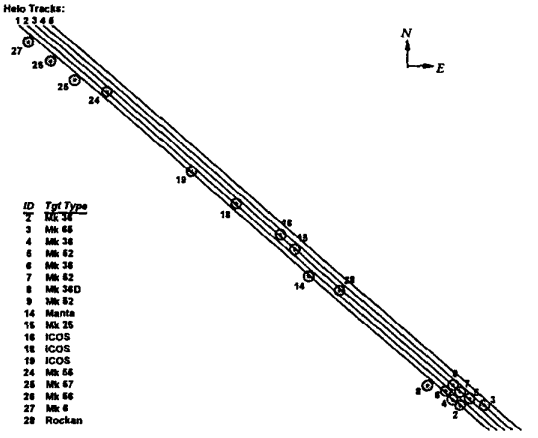

Fig. 8. CSS Panama City minefield layout

The CAD/CAC algorithm also detected several non-minelike objects and bottom features. Over the five test runs, a total of 14 such features were detected, corresponding to an exceedingly low number of false alarms per square nautical mile. Four of these cases corresponded to portions of a sunken septic tank and a clump of ladders.

Depending on the orientation of the objects relative to the sonar track, several of their echo characteristics were interpreted by CAD/CAC as being consistent with isolated mine-like regions. Note that an additional non-minelike test object (a large cable reel) was rejected on all five test trials.

Figs. 9-11 show the detailed performance of the algorithm for some of the mine target images produced by the SLS sonar. In these images circular overlays are used to indicate correct detection/classification, and rectangular overlays are used to indicate missed targets. The vertical scales represent slant range from the towed body, while the horizontal scales correspond to the tow body along-track beams.

V. REMUS CAD/CAC RESULTS

The Raytheon AN/AQS-20 CAD/CAC algorithm was modified to process REMUS imagery. These images were collected by WHOI in September 1998 in the San Diego Bay area. The first step was to account for the different image sizes between the AN/AQS-20 and REMUS. The sidescan imagery consists of images of 507 beam samples by 712 range samples. The REMUS imagery consists of 1000 rows by 512 columns. A typical REMUS image shown in Fig. 12 reveals that approximately one quarter of the range samples on either side contained pixels of poor image quality. (Note that these pixels are normally covered by the GFS in the AN/AQS-20.) Therefore the first 156 columns on both sides

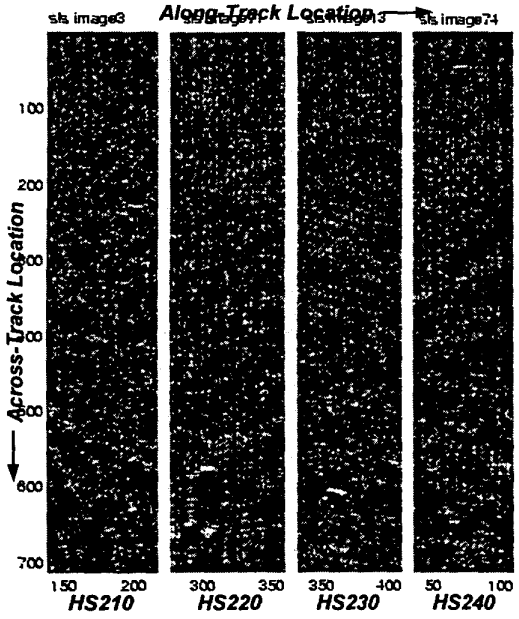

Fig. 9. Extracted images and associated CAD/CAC results for target 4

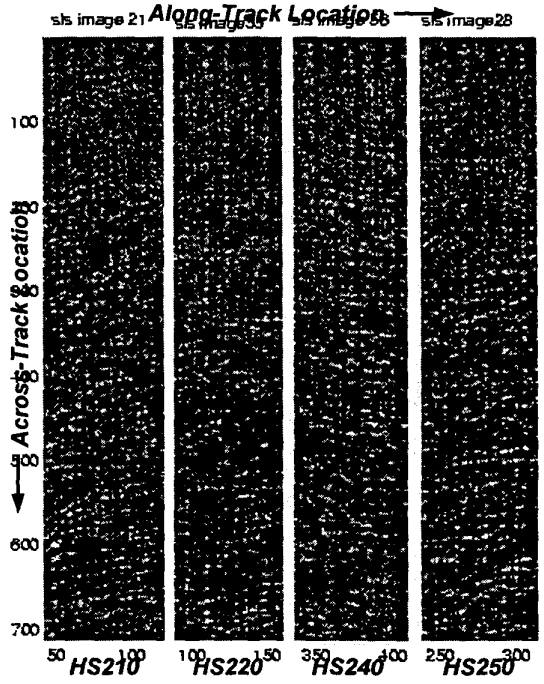

Fig. 11. Extracted images and associated CAD/CAC results for target 28

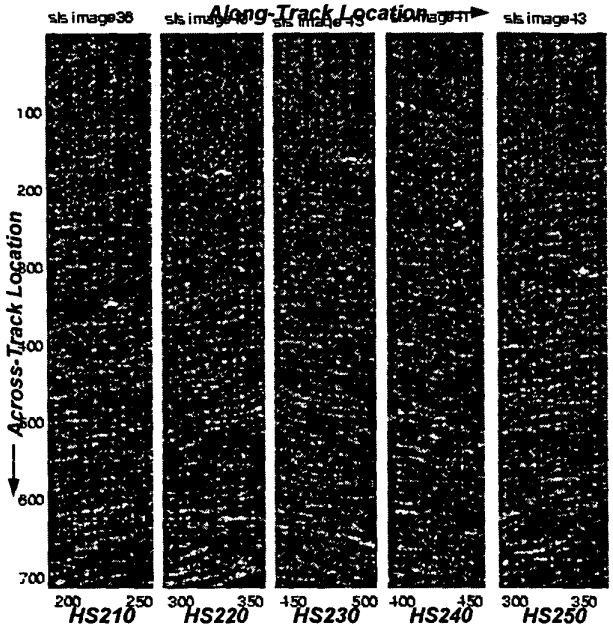

Fig. 10. Extracted images and associated CAD/CAC results for target 18

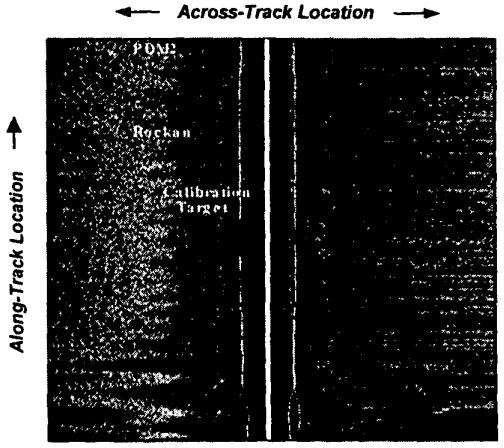

Fig. 12. Example REMUS sidescan sonar image

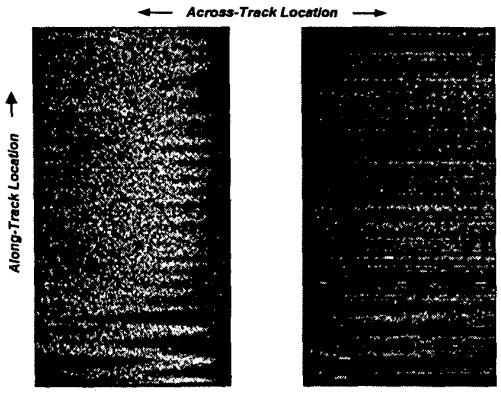

Fig. 13. REMUS image with close range pixels removed

of the image were eliminated, leaving 356 columns, which is equivalent to the first 8 range segments (or "subframes") of the Raytheon AN/AQS-20 image. After the elimination of the poorly formed pixels the same image appears in Fig. 13.

Note that to directly apply the Raytheon AN/AQS-20 CAD/CAC algorithm, 356 additional background columns were introduced by zero padding, corresponding to subframes 9 to 16. The resulting image is 1000 rows by 712 columns per side. The zero (background) padding has no effect on the CAD/CAC performance since only the highlight (brightest) and shadow (darkest) regions are considered for target detection. No detections were obtained in these zero-padded subframes (9 through 16), as expected.

Several parameter and code modifications were subsequently made to the AN/AQS-20 CAD/CAC algorithm to obtain acceptable detection performance. These changes include:

- Modifying the adaptive thresholds on the percentage of highlight and shadow pixels selected for each subframe in the image.
- Enhancing the scores of highlight regions that don't associate with shadows, since many of the REMUS targets did not have distinctive shadow regions.
- Improving the clustering of two adjacent highlight features into a single highlight region, since several targets in the REMUS images have target highlights that appear to be divided in the middle.
- Modifying the feature weighting to improve the overall scores of highlight regions.

Fig. 14 shows a sample intermediate output obtained from applying the modified CAD/CAC algorithm to the REMUS image of Fig. 13, illustrating the extracted highlight (white) and shadow (black) feature regions that are passed to the classification stage of the algorithm for final association and feature scoring. At the end of the CAD/CAC processing all three targets identified in Fig. 12 were correctly classified as being minelike. Fig. 15 shows additional examples of CAD/CAC performance on REMUS imagery.

VI. Data Fusion with REMUS Imagery

A method for combining the outputs of three different (CAD/CAC) algorithms has been developed and applied to a set of sidescan sonar data taken in the Very Shallow Water (VSW) environment, where the CAD/CAC algorithms are each tuned to detect mine-like objects [2]. The three algorithms come from Raytheon, CSS, and Lockheed Martin (LM). The fusion center receives from each algorithm the planar image coordinates and a confidence factor associated with individual CAD/CAC contacts, and produces fused classification reports of the mine-like objects. Since the three CAD/CAC algorithms use very different approaches, we have made the reasonable assumption that valid classifications are nearby each other and false alarms occur randomly in the image. The resultant geometric clustering eliminates most of the false alarms while maintaining a high level of correct classification performance. Our unique fusion algorithm takes a constrained optimization approach, which minimizes the total number of false alarms over the clustering distance and cluster confidence factor thresholds for a given probability of correct classification. Resultant receiver operating characteristics show a significant reduction in the number of false contacts: the false alarm rate from any individual CAD/CAC algorithm is reduced by a factor of four or greater through the optimized data fusion processing.

In processing the REMUS data, the various detection thresholds in our CAD/CAC algorithm are lowered substantially from their corresponding AN/AQS-20 values in order to increase the correct classification probability, relying on

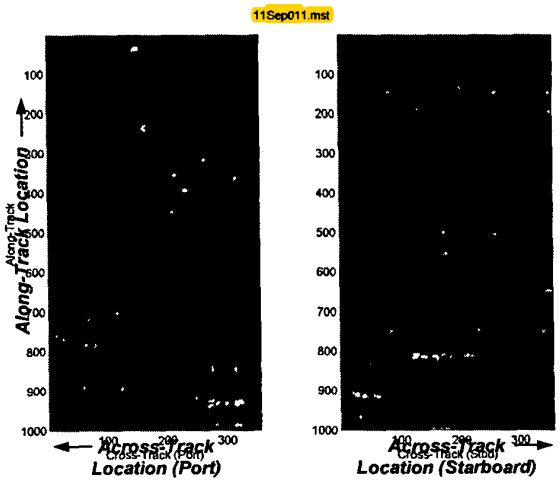

Fig. 14. Highlight and shadow regions of the REMUS image shown in Fig. 13.

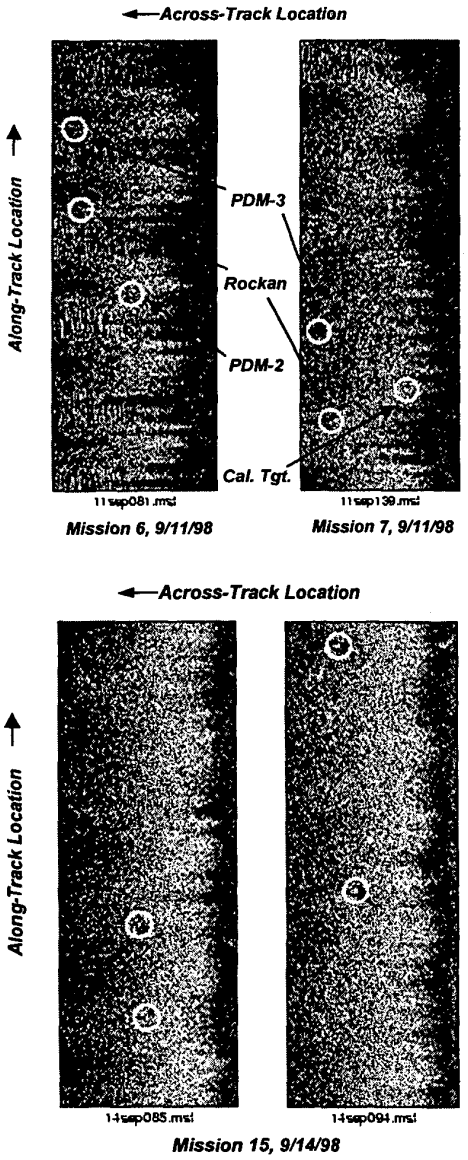

Fig. 15. CAD/CAC results on REMUS imagery

the data fusion stage to eliminate any associated increased false alarms. The introduction of a second detection/classification stage performs two functions. First, a set of CAD/CAC feature thresholds is derived, which greatly reduces the total number of false alarms. Second, a confidence factor is assigned to each CAD/CAC contact to be used for data fusion with results from the other teams. The normalized confidence factor is a linear combination of the CAD/CAC score and the feature signal to noise ratio (SNR) for the contact. The weighting in the linear combination is chosen so that valid detections tend to have high confidence factors (approaching 1.0), while false alarms tend to have low confidence factors (approaching 0.5).

Fig. 16 illustrates the various stages of data processing required to obtain the data fusion result. First, an image is processed by the Raytheon CAD/CAC algorithm. The resulting CAD/CAC contacts are processed by a second stage classification algorithm which performs threholding on the features of the CAD/CAC contacts for false alarm reduction. In the third step, the confidence factor for each CAD/CAC contact is calculated. In addition, image coordinates compatible with a standardized image coordinate system are produced via a coordinate transformation, so that the CAD/CAC contacts from the three teams are geometrically consistent with each other. Next, the CAD/CAC results from all teams participating in the fusion process are collected for geometric clustering. The resulting CAD/CAC clusters and cluster confidence factors are then processed via cluster confidence factor thresholding to produce the final fused result, which consists of the cluster position (centroid of CAD/CAC contacts within the cluster) and the cluster confidence factor.

The individual CAD/CAC algorithms provide the data fusion process with the image coordinates of CAD/CAC contacts and their associated confidence factors. Since there are three teams (CSS, Lockheed Martin, Raytheon) contributing to the data fusion, four types of data fusion were tested: fusing the results of CSS and Lockheed Martin, fusing the results of CSS and Raytheon, fusing the results of Lockheed Martin and Raytheon, and fusing the results of all three teams. Furthermore, for each of the four types of fusion there are two methods of geometric clustering:

1. ***Euclidean clustering.*** The square root of the sum of the squared distances in the along-track (x) and cross-track (y) directions are used for the clustering criterion: two CAD/CAC contacts belong to the same cluster if the Euclidean distance between them is less than some threshold T_e.
2. ***X-Y clustering.*** The along-track and cross-track distances are used as two separate clustering criteria: two CAD/CAC contacts are in the same geometric cluster if they are less than some clustering threshold T_x away in the along-track distance and some clustering threshold T_y away in the cross-track distance.

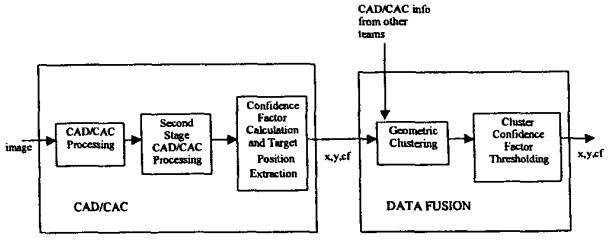

Fig. 16. Data fusion processing chain

In both algorithms, no team can have more than one element in a cluster, and the cluster is assigned a cluster confidence factor, that is the minimum of all the individual confidence factors in the cluster. A standard algorithm[4] that generates equivalence classes is used to perform the geometric clustering.

Upon the completion of the geometric clustering, the following clusters were discarded in the case of three team data fusion: clusters containing only one CAD/CAC contact, clusters containing one contact from CSS and one contact from Lockheed Martin whose cluster confidence factor is lower than some threshold T_{cl}, clusters containing one contact from CSS and one contact from Raytheon whose cluster confidence factor is lower than some threshold T_{cr}, clusters containing one contact from Lockheed Martin and one contact from Raytheon whose cluster confidence factor is lower than some threshold T_{lr}, and clusters containing contacts from all three teams whose cluster confidence factor is lower than some threshold T_{clr}.

In the case of two team data fusion (e.g., CSS and Raytheon), we discard clusters with only one CAD/CAC contact and clusters with two CAD/CAC contacts whose confidence factor is lower than some threshold (e.g. T_{cr}).

The thresholds T_e, T_x, T_y, T_{cl}, T_{cr}, T_{lr}, T_{clr} are dependent on the desired probability of correct classification and derived by a constrained optimization approach. For example, in three team fusion, using Euclidean geometric clustering, we perform the following procedure:

1. Fix T_e. (Note that initially one can use the maximum distance between valid detections over all targets for T_e).
2. Find the values of T_{cl}, T_{cr}, T_{lr}, T_{clr} that yield the fewest total number of false alarms for the desired probability of classification.
3. Change the value of T_e.
4. Repeat.

After a sufficient number of different values for T_e are tried, the 5-tuple (T_e, T_{cl}, T_{cr}, T_{lr}, T_{clr}) which yields the fewest number of total false alarms comprises the set of thresholds for the desired probability of classification. In this manner a Receiver Operating Characteristics (ROC) curve can be generated, where each point on the curve corresponds to a different set of five thresholds.

Figs. 17 and 18 show the Receiver Operating Characteristics (ROC) plots for the Euclidean and X-Y methods of clustering. Each point on the ROC curves correponds to a different set of cluster confidence factor thresholds. Note that the optimal fusion algorithm reduces the false alarm rate to 0.1 per image per side at a 90% correct classification probability. This false alarm rate is approximately 1/4 that of the best performing single CAD/CAC algorithm.

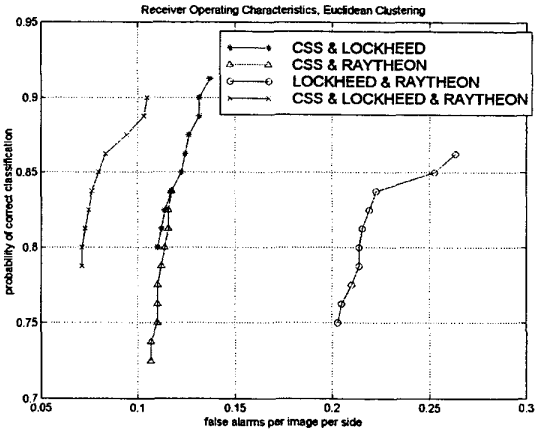

Fig. 17. ROC plots for Euclidean clustering

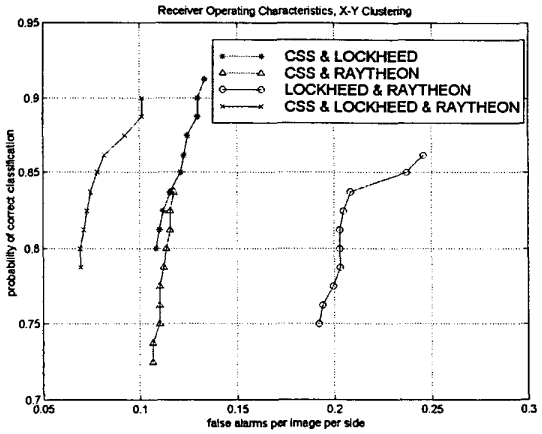

Fig. 18. ROC plots for X-Y clustering

VII. SUMMARY

Raytheon's CAD/CAC processing has been demonstrated to provide an operationally significant capability for the detection and classification of bottom mines. It provides an attractive alternative and/or supplement to current approaches, which use diver/mammal teams to identify underwater mines. Use of CAD/CAC allows the mine reconnaissance mission to be performed onboard a helicopter or remotely by the REMUS vehicle, removing the diver/mammal teams from the hazards posed by mines, while reducing the time required for locating mines. An underwater autonomous

vehicle such as REMUS also has the added advantage of enhancing operation covertness. Furthermore, it has been demonstrated that the original AN/AQS-20 CAD/CAC algorithm is flexible enough to process imagery taken by different vehicles in different environments, with only minor modifications.

In addition, we presented a data fusion algorithm, which clearly shows the benefits of combining the outputs of diverse CAD/CAC algorithms, providing greater than 4:1 reduction in false alarms over any single algorithm. As expected, the valid classifications from the three algorithms tended to cluster together, while the majority of the false alarms did not. The latter became clusters containing only one element, and therefore were discarded. It is important to note that this fusion approach requires very little communication bandwidth, since each team provides only the location and the confidence factor of its CAD/CAC contacts.

ACKNOWLEDGEMENTS

The authors would like to acknowledge both the CSS and Raytheon AN/AQS-20 engineering teams, who have supported the system development with steadfast effort. Special acknowledgments go to the CSS AN/AQS-20 team leader, Vickie Seldenright of Code A21, for her dedicated efforts in coordinating all test activities, and Program Executive Office Airborne Mine Defense (PMS-210) for sponsoring the AN/AQS-20 program.

The authors also gratefully acknowledge Dr. Thomas Swean of the Ofifice of Naval Research (ONR) for supporting the REMUS CAD/CAC and data fusion studies, as well as Dr. Gerald J. Dobeck of the NSWC Coastal Systems Station, Dahlgren Division, Panama City, Florida, who provided helpful technical discussions and overall project coordination.

REFERENCES

[1] Johnson, S. G. & Deaett, M. A., "The Application of Automated Recognition Techniques to Side-Scan Sonar Imagery," *IEEE J. Oceanic Engineering*, 19, No. 1, 138-144, January 1994.

[2] Huang, J., Ciany, C., Broadman, M. & Doran, S., "Data fusion of computer aided detection/computer aided classification algorithms for classification of mines in very shallow water environments," *Proceedings of the SPIE*, Vol. 4038, April 24-28, 2000.